Performance Enhanced Coded OFDM with Almost Linear Interleaver over Rayleigh Fading Channels

Chenggao Han and Takeshi Hashimoto

Graduate School of Informatics and Engineering,

The University of Electro-Communications

1-5-1 Chofugaoka, Chofu-shi, Tokyo 185-8585, Japan

E-mail: han.ic@uec.ac.jp

Abstract

This paper presents a comprehensive performance analysis of *coded orthogonal frequency division multiplexing* (COFDM) over the quasi-static multipath Rayleigh fading channels. We first analyze the *pairwise error probability* (PEP) of COFDM and then consider the union bound on *bit error rate* (BER) by introducing the notion of *diversity guard* (DG) and a novel interleaver class, named *almost linear interleaver* (ALI). A construction of ALI is also introduced with its parameter selection. Simulation results show that the COFDM with ALI outperforms that with *random interleaver* (RI) and the *block interleaver* (BI) adopted in the IEEE industry standards.

Index Terms

coded OFDM (COFDM), frequency diversity, diversity order, convolutional code, interleaver design.

I. INTRODUCTION

Orthogonal frequency division multiplexing (OFDM) has been used to provide *inter-symbol interference* (ISI)-free transmission [1]–[4] with simple receiver structure in multipath environment and is widely accepted in many industry standards such as ADSL, WLAN, WiMAX, and digital TV. However, since the pure OFDM system is lacking for obtaining diversity gain, the *coded OFDM* (COFDM) scheme is extensively used in practical applications [5]–[7]. In COFDM, the information bits are coded with an error correcting code and the resultant codeword is interleaved over subcarriers. If a *convolutoinal code* (CC) with free distance d_f is employed for COFDM, with a properly designed interleaver, COFDM potentially achieves diversity of order $\min\{P, d_f\}$ over a P-path multipath fading channel. Ahthough the performance of COFDM has been analyzed by numerous researchers *e.g.*, [8], [9], little attention has been given to the role of interleaver and its design for COFDM.

Interleaver has wide application in error correcting codes, such as CC, Turbo code, Reed-Solomon code, *etc.*, and in the practical applications of COFDM, it plays an important role for the maximization of diversity order and coding gain. However, to find the desired interleaver for a specific code, exhaustive searching of all the possibilities is of course an impossible task. Therefore, the *random interleaver* (RI) that is designed in a pseudorandom manner is popularly considered for research purposes and, to prevent adjacent bits being mapped to positions in a short Hamming distance, *semi-random interleavers* (S-RIs) [10] and its modifications [11], [12] are also used. However, since RI requires extra memories to store look-up tables, for a large block size, it is storage-expensive and is difficult to implement the extra property such as contention-free property [13].

Among deterministic interleavers, the *block interleaver* (BI) [14] and *linear interleaver* (LI) [15] are two simple interleavers. For the interleaver size L, a BI of depth D exists if $\gcd(L, D) = D$ while a LI of depth D exists if $\gcd(L, D) = 1$[1]. We may properly design BIs and LIs which perform better than RIs for a small L but for medium to large frame sizes in general. Therefore, to improve the performance of turbo codes for a large frame size, interleaver design for a large L has been extensively studied by many researchers. The *almost regular permutation* (ARP) [16] and *quadratic permutation polynomial* (QPP) interleavers [17], [18] are such examples and the QPP is selected for the *Long term evaluation* (LTE) standard [19]. However, QPP is designed for the tail-biting Turbo code for AWGN channel. For COFDM, IEEE adopted the depth-$QN/16$ BI in the industry standards 802.11a [20] and IEEE 802.16e [21], where N and 2^Q are the numbers of subcarriers and constellation size, respectively. We have been shown in [22] that the performance of COFDM can be improved by the use of a novel interleaver class, named *almost linear interleaver* (ALI).

This paper presents a thorough study of the COFDM with ALI. We analyze the *bit error rate* (BER) performance and consider the interleaver design problem of COFDM over multipath Rayleigh fading channels. Under assumption of the QPSK with Gray labeling and the *maximum likelihood* (ML) decision, we obtain a union (upper-)bound on BER from *pair-wise error probability* (PEP). After than, we introduce the notions of *diversity guard* (DG) to the interleavers which guarantee the diversity of order d_f for the codewords of weight $d_f + G$, for a certain $G > 0$. For simplification of the union bound, we confine our attention to ALIs which make the union bound is irrelevant to the starting position of codeword errors. Subsequently, a construction of ALI is introduced with its parameter selection for COFDM applications over multipath fading

[1] $\gcd(L, D)$ denotes the greatest common divisor between L and D.

channels. After verifying the validity of the approximation utilized in the simplification, we performed computer simulations for COFDM systems with 64 and 1024 subcarriers employing CCs adopted in IEEE 802.11a and IEEE 802.16e over the quasi-static multipath Rayleigh fading channels. The simulation results shown that the COFDM with ALI always outperforms that with RI and the BI adopted in the IEEE 802.11a and IEEE 802.16e standards.

The rest of this paper is organized as follows. In Section II, we briefly review COFDM. Section III introduces an upper bound of PEP for COFDM over quasi-static multipath Rayleigh fading channels under assumption of the *maximum likelihood* (ML) decision. In Section IV, we derive a union bound on BER and its simplification. A construction ALI is proposed in Section V with its parameter selection and the conjecture utilized for the simplification of the union bound is verified in Section VI. Simulaiton results are shown in Section VII. Finally, we conclude this paper in Section Section VIII.

A. *Notations*

Throughout the paper, we assume the following notations. For a random variable ξ, $E\{\xi\}$ expresses the expectation of ξ. For two integers a and b, $\lfloor a/b \rfloor$ denotes the maximum integer not greater than a/b while the minimum integer not smaller than a/b is denoted by $\lceil a/b \rceil$. $[a]_b$ is nonnegative integer less than b satisfying $(a - [a]_b) \mod b = 0$. For a finite set $\mathcal{A}$, its size is denoted by $|\mathcal{A}|$. For two sets $\mathcal{A}$ and $\mathcal{B}$, their union and intersection are denoted by $\mathcal{A} \cup \mathcal{B}$ and $\mathcal{A} \cap \mathcal{B}$, respectively, and $\mathcal{A} \backslash \mathcal{B} := \{a \in \mathcal{A} | a \notin \mathcal{B}\}$. For a complex number x, its real part and its conjugate is denoted by $\Re\{x\}$ and x^*, respectively. Vectors and matrices are denoted by a bold latter. Given a length-L row vector $\boldsymbol{x} = (x_0, x_1, \cdots, x_{L-1})$ which is some times written as $(x_\ell)_{\ell=0}^{L-1}$ and $(x_\ell)_{\ell \in \mathcal{L}}$ denotes the length-$|\mathcal{L}|$ vector consisting of the elements x_ℓ, $\ell \in \mathcal{L}$. The Euclidean norm of $\boldsymbol{x}$ is denoted by $\|\boldsymbol{x}\|$, and $\mathrm{diag}(x_\ell)_{\ell=0}^{L-1}$ denotes a diagonal matrix with the ℓth diagonal entry x_ℓ. A length-v all-zero (-one) vector is denoted by $\mathbf{0}_v$ ($\mathbf{1}_v$). An $M \times N$ matrix $\boldsymbol{X}$ is denoted in terms of its (m,n)th entry as $[x_{m,n}]_{m=0,n=0}^{M-1,N-1}$ or simply $[x_{m,n}]$ if its size is obvious. Given $\boldsymbol{X}$, its mth row is denoted by $\boldsymbol{x}_m = (x_{m,0}\ x_{m,1}\ \cdots\ x_{m,N-1})$ and $[x_{m,n}]_{m\in\mathcal{M},n\in\mathcal{N}}$ denotes the size $|\mathcal{M}| \times |\mathcal{N}|$ matrix consisting of entries $x_{m,n}$ for $m \in \mathcal{M}$ and $n \in \mathcal{N}$. $\boldsymbol{X}^T$ and $\boldsymbol{X}^H$ denotes the transpose and complex conjugate transpose of $\boldsymbol{X}$, respectively. The size $N \times N$ identity matrix is denoted by $\boldsymbol{I}_N$ and the N-dimensional discrete Fourier transform (DFT) matrix is an $N \times N$ matrix $\boldsymbol{F}_N = [W_N^{mn}]$ for $W_N = \exp(-2j\pi/N)$. Then, the N-dimensional inverse discrete Fourier transform (IDFT) matrix is $\boldsymbol{F}_N^{-1} = [W_N^{-mn}]/N$.

II. Review of COFDM

The block diagram of the COFDM system with N subcarriers is shown in Fig. 1. The

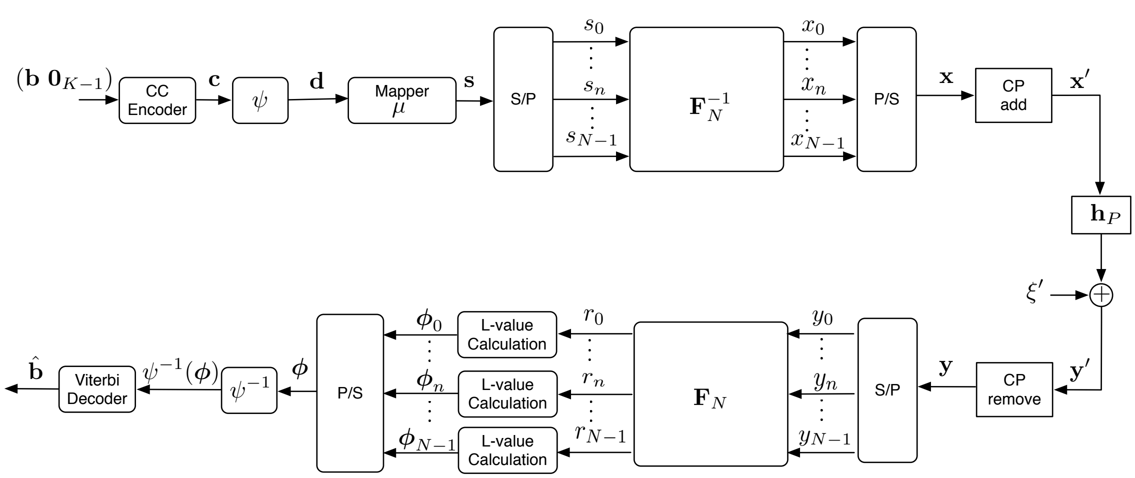

Fig. 1. Block diagram of COFDM

information vector $(\boldsymbol{b}\ \mathbf{0}_{K-1}) \in \{0,1\}^{RL}$ terminated with an $\mathbf{0}_{K-1}$ for $\boldsymbol{b} \in \{0,1\}^{RL-K-1}$ is encoded by a rate-R binary CC $\mathcal{C}$ with constraint length K to give a length-L *codeword* $\boldsymbol{c} \in \mathcal{C}$ for $L = QN$, $Q > 0$. The initial state of the encoder is assumed to be $\mathbf{0}_{K-1}$. Next, $\boldsymbol{c}$ is fed to an interleaver Ψ to give the *interleaved codeword* (ICW) $\boldsymbol{d} = (d_\ell)_{\ell=0}^{L-1} = \Psi(\boldsymbol{c})$, and $\boldsymbol{d}$ is partitioned into N length-Q subsequences $\boldsymbol{d}_n := (d_{n,q})_{q=0}^{Q-1}$ for $d_{n,q} = d_{nQ+q}$, $0 \le n < N$. Each $\boldsymbol{d}_n$ is then mapped to a point of the signal constellation[2] $\mathcal{S}$, $\mu(\boldsymbol{d}_n) \in \mathcal{S}$, and the resultant *symbol vector* $\boldsymbol{s} = \mu(\boldsymbol{d}) = (\mu(\boldsymbol{d}_n))_{n=0}^{N-1}$ is transformed to a time-domain signal vector $\boldsymbol{x} = \boldsymbol{s}\boldsymbol{F}_N^{-1}$ by size-N IDFT. Finally, a length-N_G *cyclic prefix* (CP) is appended to $\boldsymbol{x}$ and the resultant time domain signal $\boldsymbol{x}' = \left(x_{[n]_N}\right)_{n=-N_G}^{N-1}$ is transmitted over the channel.

Let $\boldsymbol{h}_P := (h_p)_{p=0}^{P-1}$ be the channel impulse response and we assume quasi-static Rayleigh fading, that is, h_p are mutually independent complex-valued *circularly symmetric* (CS) Gaussian random variables [23] with $E\{h_p\} = 0$ and $E\{|h_p|^2\} = \sigma_p^2 > 0$ for $0 \le p < P$. Thus, $E\{\boldsymbol{h}_P^H \boldsymbol{h}_P\} = \boldsymbol{\Sigma}_P := \operatorname{diag}\left(\sigma_p^2\right)_{p=0}^{P-1}$. The channel is corrupted by complex-valued *additive white Gaussian noise* (AWGN) $\boldsymbol{\xi}$ with $E\{\boldsymbol{\xi}\} = 0$ and $E\{\boldsymbol{\xi}^H \boldsymbol{\xi}\} = (N_0/N)\boldsymbol{I}_N$.

At the receiver, after the CP removed, the length-N received signal $\boldsymbol{y}$ is transformed by DFT to a frequency domain vector $\boldsymbol{r} = \boldsymbol{y}\boldsymbol{F}_N$. Thus, if we let $\boldsymbol{\eta} := \boldsymbol{\xi}\boldsymbol{F}_N$ and $\tilde{\boldsymbol{h}} := \boldsymbol{h}\boldsymbol{F}_N$ for $\boldsymbol{h} = (\boldsymbol{h}_P\ \boldsymbol{0}_{N-P})$, OFDM provides a frequency-domain channel model

$$\boldsymbol{r} = \boldsymbol{s}\operatorname{diag}(\tilde{\boldsymbol{h}}) + \boldsymbol{\eta}$$

We assume that the channel vector $\boldsymbol{h}$ and the noise variance N_0 are known at the receiver. For decoding the transmitted information, assuming all $d_{n,q}$ are equiprobable, we introduce the *log-likelihood ratio* (LLR) of $d_{n,q}$ as

$$\begin{aligned}
\phi_{n,q} &= \ln \frac{\Pr\{d_{n,q} = 1|\boldsymbol{r}\}}{\Pr\{d_{n,q} = 0|\boldsymbol{r}\}} \\
&= \ln \frac{\sum_{\boldsymbol{z}\in\{0,1\}^Q|z_q=1} \exp\left(\frac{-|r_n - \mu(\boldsymbol{z})\tilde{h}_n|^2}{N_0}\right)}{\sum_{\boldsymbol{z}\in\{0,1\}^Q|z_q=0} \exp\left(\frac{-|r_n - \mu(\boldsymbol{z})\tilde{h}_n|^2}{N_0}\right)}
\end{aligned}$$

[2]The binary vector $\boldsymbol{d}_n$ is labeling of the symbol $\mu(\boldsymbol{d}_n)$.

Let $\boldsymbol{\phi}_n := (\phi_{n,q})_{q=0}^{Q-1}$, $\boldsymbol{\phi} := (\boldsymbol{\phi}_n)_{n=0}^{N-1}$, and $\boldsymbol{\rho} := \Psi^{-1}(\boldsymbol{\phi})$. Then, from $\rho_\ell = \ln\left[\Pr\{c_\ell = 1|\boldsymbol{r}\}/\Pr\{c_\ell = 0|\boldsymbol{r}\}\right]$, we have $\Pr\{c_\ell = x|\boldsymbol{r}\} = x\rho_\ell - \ln[1+\exp(\rho_\ell)]$ for $x \in \{0,1\}$. Thus, we recover the transmitted information by the minimization

$$\hat{\boldsymbol{b}} = \underset{\boldsymbol{b}\in\{0,1\}^{QNR-K-1}}{\arg\min} \sum_{\ell=0}^{QN-1} \left\{\ln[1+\exp(\rho_\ell)] - \rho_\ell c_\ell(\boldsymbol{b})\right\},$$

where $c_\ell(\boldsymbol{b})$ is the ℓth bit of the codeword corresponding to $\boldsymbol{b}$ and the decision (1) is carried out with the *Viterbi algorithm*.

We consider QPSK modulation ($Q = 2$) for $\mathcal{S} = \{\pm 1, \pm j\}$ with the Gray labeling

$$\begin{cases} \mu((00)) &= 1 \\ \mu((01)) &= j \\ \mu((10)) &= -j \\ \mu((11)) &= -1 \end{cases}$$

Since $d_{n,q}$ are equiprobable, all the symbols in $\mathcal{S}$ are selected with equal probability.

In general, the decoding rule (1) may not meet the *maximum likelihood* (ML) decision criterion. However, the following theorem is proved in Appendix A.

Theorem 1. For the QPSK modulation[3] with Gray labeling given in (2), the decision rule (1) provides ML decision.

III. Pair-wise error probability

For the transmitted symbol vector $\boldsymbol{s} \in \mathcal{S}^N$, a detection error occurs if an erroneous $\boldsymbol{s}' \in \mathcal{S}^N$, $\boldsymbol{s}' \neq \boldsymbol{s}$, is selected. Let $\boldsymbol{e} := \boldsymbol{s} - \boldsymbol{s}'$ be the *symbol error vector* (SEV) relative to $\boldsymbol{s}$ and let $P(\boldsymbol{e}\,|\boldsymbol{s})$ be the *pair-wise error probability* (PEP) that the transmitted $\boldsymbol{s}$ has less likelihood than $\boldsymbol{s}' = \boldsymbol{s} - \boldsymbol{e}$.

[3]Trivally holds for BPSK too.

A. PEP bound in terms of SEV

For a given $\tilde{\boldsymbol{h}}$, the probability that the symbol $\boldsymbol{s}' = \boldsymbol{s} - \boldsymbol{e}$ has a likelihood larger than $\boldsymbol{s}$ is bounded as

$$\begin{aligned} P\left(\boldsymbol{e}\middle|\tilde{\boldsymbol{h}}\right) &\leq \Pr\left(\|\boldsymbol{r} - \boldsymbol{s}\,\mathrm{diag}(\tilde{\boldsymbol{h}})\|^2 \geq \|\boldsymbol{r} - \boldsymbol{s}'\,\mathrm{diag}(\tilde{\boldsymbol{h}})\|^2 \middle| \tilde{\boldsymbol{h}}\right) \\ &= \Pr\left(2\Re\left\{\boldsymbol{e}\,\mathrm{diag}(\tilde{\boldsymbol{h}})\boldsymbol{\eta}^H\right\} \leq -\left\|\boldsymbol{e}\,\mathrm{diag}(\tilde{\boldsymbol{h}})\right\|^2 \middle| \tilde{\boldsymbol{h}}\right) \end{aligned}$$

Since $\Re\left\{\boldsymbol{e}\,\mathrm{diag}(\tilde{\boldsymbol{h}})\boldsymbol{\eta}^H\right\}$ has a Gaussian distribution with mean zero and variance $N_0\left\|\tilde{\boldsymbol{h}}\,\mathrm{diag}\left(\boldsymbol{e}\right)\right\|^2/2$, the conditional PEP is bounded as

$$P\left(\boldsymbol{e}\middle|\tilde{\boldsymbol{h}}\right) \leq Q\left(\sqrt{\frac{\left\|\tilde{\boldsymbol{h}}\,\mathrm{diag}(\boldsymbol{e})\right\|^2}{2N_0}}\right) = \frac{1}{\pi}\int_0^{\frac{\pi}{2}} \exp\left\{-\frac{\|\tilde{\boldsymbol{h}}\,\mathrm{diag}(\boldsymbol{e})\|^2}{4N_0\sin^2\alpha}\right\} d\alpha$$

where $Q(x)$ is the Gaussian Q-function and the Craig's Q-function expression is used [24], [25].

For an SEV $\boldsymbol{e} = (e_n)_{n=0}^{N-1}$, let $\mathcal{N}(\boldsymbol{e}) := \{n\,|e_n \neq 0, 0 \leq n < N\}$ and call it the *symbol support set* (SSS) of $\boldsymbol{e}$. As discussed in [26], the covariance matrix of $\tilde{\boldsymbol{h}}$ takes different forms depending on whether $|\mathcal{N}(\boldsymbol{e})| > P$ or $|\mathcal{N}(\boldsymbol{e})| \leq P$. The case $|\mathcal{N}(\boldsymbol{e})| > P$ is true either if there are many symbol errors or if P is small. The occurrence of many symbol errors is considered to be rare in general. The occurrence of a small P is, on the other hand, considered to be an indication of of small path loss as discussed in [27], [28]. Thus, in this paper, we consider the case $|\mathcal{N}(\boldsymbol{e})| \leq P$.

For a given $\boldsymbol{e}$, let $\bar{\boldsymbol{h}}(\boldsymbol{e}) := \left(\tilde{h}_n\right)_{n\in\mathcal{N}(\boldsymbol{e})}$. Then, we have $\left\|\tilde{\boldsymbol{h}}\,\mathrm{diag}(\boldsymbol{e})\right\|^2 = \left\|\bar{\boldsymbol{h}}(\boldsymbol{e})\,\mathrm{diag}(e_n)_{n\in\mathcal{N}(\boldsymbol{e})}\right\|^2$. For $|\mathcal{N}(\boldsymbol{e})| \leq P$, the correlation matrix of the random vector $\bar{\boldsymbol{h}}(\boldsymbol{e})$ is given by

$$\boldsymbol{D}(\boldsymbol{e}) = E\left\{\bar{\boldsymbol{h}}(\boldsymbol{e})^T\bar{\boldsymbol{h}}^*(\boldsymbol{e})\right\} = \left[\sum_{p=0}^{P-1} W_N^{(n-n')p}\sigma_p^2\right]_{n\in\mathcal{N}(\boldsymbol{e}),n'\in\mathcal{N}(\boldsymbol{e})}$$

Since $\sigma_p^2 > 0$ for $0 \leq p < P$, the Hermitian matrix $\boldsymbol{D}(\boldsymbol{e})$ is non-singular, and the PEP bound is averaged with respect to the probability of $\bar{\boldsymbol{h}}(\boldsymbol{e})$ as follows

$$\begin{aligned}
P(\boldsymbol{e}) &= E_{\tilde{\boldsymbol{h}}}\left\{P(\boldsymbol{e}|\tilde{\boldsymbol{h}})\right\} \\
&= \frac{1}{\pi^{|\mathcal{N}(\boldsymbol{e})|}\det(\boldsymbol{D}(\boldsymbol{e}))}\int P\left(\boldsymbol{e}\,|\boldsymbol{x}\right)\exp\left(-\boldsymbol{x}\boldsymbol{D}^{-1}(\boldsymbol{e})\boldsymbol{x}^H\right)d\boldsymbol{x} \\
&\leq \frac{1}{\pi^{|\mathcal{N}(\boldsymbol{e})|+1}\det(\boldsymbol{D}(\boldsymbol{e}))}\int_0^{\frac{\pi}{2}}\left\{\int\exp\left(-\frac{\boldsymbol{x}\boldsymbol{D}(\boldsymbol{e})\boldsymbol{x}^H}{4N_0\sin^2\alpha}\right)d\boldsymbol{x}\right\}d\alpha \\
&= \frac{1}{\pi}\int_0^{\frac{\pi}{2}}\frac{(4N_0)^{|\mathcal{N}(\boldsymbol{e})|}\sin^{2|\mathcal{N}(\boldsymbol{e})|}\alpha}{\det(\boldsymbol{B}(\boldsymbol{e},\alpha)\boldsymbol{D}(\boldsymbol{e}))}\,d\alpha,
\end{aligned}$$

where we let $\boldsymbol{B}(\boldsymbol{e},\alpha) := \mathrm{diag}\left(|e_n|^2\right)_{n\in\mathcal{N}(\boldsymbol{e})} + 4N_0\left(\sin^2\alpha\right)\boldsymbol{D}^{-1}(\boldsymbol{e})$. If we substitute $\det\left(\boldsymbol{B}(\boldsymbol{e},\alpha)\right) \geq \prod_{n\in\mathcal{N}(\boldsymbol{e})}|e_n|^2$ and calculate the integral with respect to α, then we have a simper upper-bound

$$P(\boldsymbol{e}) \leq \frac{{}_{2|\mathcal{N}(\boldsymbol{e})|-1}C_{|\mathcal{N}(\boldsymbol{e})|-1}N_0^{|\mathcal{N}(\boldsymbol{e})|}}{\det\left(\boldsymbol{D}(\boldsymbol{e})\right)\prod_{n\in\mathcal{N}(\boldsymbol{e})}|e_n|^2},$$

where ${}_nC_r$ is the binomial coefficient.

B. PEP bound in terms of codeword error vectors

For distinct codewords $\boldsymbol{c}, \boldsymbol{c}' \in \mathcal{C}$, we call $\boldsymbol{\iota}(\boldsymbol{c}) := \boldsymbol{c} \oplus \boldsymbol{c}'$ the *codeword error vector* (CWEV) relative to $\boldsymbol{c}$, where $\oplus$ denotes component-wise exclusive-OR addition. From the linearity of CC, $\boldsymbol{\iota}(\boldsymbol{c})$ is a member of the set of non-zero codewords $\mathcal{E} := \mathcal{C} \setminus \boldsymbol{0}_L$ and can be a CWEV relative to any other $\boldsymbol{c}'' \in \mathcal{C}$. Thus, we simply write the CWEV as $\boldsymbol{\iota}$. If we let ICWEV $\boldsymbol{\nu} = \boldsymbol{d} \oplus \boldsymbol{d}'$ for the ICW $\boldsymbol{d} = \Psi(\boldsymbol{c})$ and $\boldsymbol{d}' = \Psi(\boldsymbol{c}')$, then apparently $\boldsymbol{\nu} = \Psi(\boldsymbol{\iota})$.

We next consider the relationship between ICWEV $\boldsymbol{\nu}$ and SEV $\boldsymbol{e} = \boldsymbol{s} - \boldsymbol{s}'$ for $\boldsymbol{s} = \mu(\boldsymbol{d})$ and $\boldsymbol{s}' = \mu(\boldsymbol{d}')$. The Gray mapping from $\boldsymbol{d}_n = (d_{n,0}, d_{n,1})$ to s_n is represented as

$$s_n = \mu\left(\boldsymbol{d}_n\right) = \frac{1}{2}\left[(-1)^{d_{n,1}} + (-1)^{d_{n,0}}\right] + \frac{j}{2}\left[(-1)^{d_{n,1}} - (-1)^{d_{n,0}}\right]$$

Thus, the squared-magnitude of the symbol error e_n is, with some abuse of logical and integer arithmetic, given as

$$|e_n|^2 = 2\left(d_{n,1} \oplus d'_{n,1} + d_{n,0} \oplus d'_{n,0}\right) = 2w_H(\boldsymbol{\nu}_n)$$

where $\boldsymbol{\nu}_n$ is the nth subsequence of $\boldsymbol{\nu}$ and $w_H(\boldsymbol{\nu}_n)$ stands for the Hamming weight of $\boldsymbol{\nu}_n$.

Since $e_n = 0$ if and only if $\boldsymbol{\nu}_n = \mathbf{0}_Q$, $\mathcal{N}(\boldsymbol{e}) = \{n | \boldsymbol{\nu}_n \neq \mathbf{0}_Q, 0 \leq n < N\}$. Thus, we also write $\mathcal{N}(\boldsymbol{e})$ as $\mathcal{N}(\boldsymbol{\nu})$. Then, the matrix $\boldsymbol{D}(\boldsymbol{e})$ is also written as

$$\boldsymbol{D}(\boldsymbol{\nu}) := \left[\sum_{p=0}^{P-1} W_N^{(n-n')p} \sigma_p^2 \right]_{n \in \mathcal{N}(\boldsymbol{\nu}), n' \in \mathcal{N}(\boldsymbol{\nu})} = \boldsymbol{D}(\boldsymbol{e})$$

and the bound (3) can be rewritten as

$$P(\boldsymbol{\nu}) \quad \leq \quad \frac{{}_{2|\mathcal{N}(\boldsymbol{\nu})|-1}C_{|\mathcal{N}(\boldsymbol{\nu})|-1} N_0^{|\mathcal{N}(\boldsymbol{\nu})|}}{\det(\boldsymbol{D}(\boldsymbol{\nu})) \prod_{n \in \mathcal{N}(\boldsymbol{\nu})} 2 w_H(\boldsymbol{\nu}_n)}$$

We note that the right-hand side of (5) is completely determined by $\boldsymbol{\nu} = \Psi(\boldsymbol{\iota})$ and can be written in the form of $[\gamma \zeta(\boldsymbol{\nu})]^{-|\mathcal{N}(\boldsymbol{\nu})|}$ for SNR $\gamma := \frac{1}{|\mathcal{S}| N_0} \sum_{s \in \mathcal{S}} |s|^2$, where $|\mathcal{N}(\boldsymbol{\nu})|$ gives the *diversity order* and $\zeta(\boldsymbol{\nu})$ defined as

$$\zeta(\boldsymbol{\nu}) \quad := \quad 2 \left(\frac{{}_{2|\mathcal{N}(\boldsymbol{\nu})|-1}C_{|\mathcal{N}(\boldsymbol{\nu})|-1}}{\det(\boldsymbol{D}(\boldsymbol{\nu})) \prod_{n \in \mathcal{N}(\boldsymbol{\nu})} w_H(\boldsymbol{\nu}_n)} \right)^{-1/|\mathcal{N}(\boldsymbol{\nu})|}$$

gives the *coding gain* of $\boldsymbol{\nu}$, respectively. In a moderate SNR region, the inclination of the PEP v.s. SNR curve is determined by the diversity order while the vertical position of the curve is determined by the coding gain [23]. Thus, in a moderate to high SNR region, we should preferentially optimize the diversity order rather than coding gain.

IV. Union bound on BER and its approximations

For the codewords $\boldsymbol{c}$ and $\boldsymbol{c}'$ whose corresponding information vectors are $\boldsymbol{b}$ and $\boldsymbol{b}'$, respectively, let $A(\boldsymbol{c}, \boldsymbol{c}') = w_H(\boldsymbol{b} - \boldsymbol{b}')$. If we let $P(\boldsymbol{c}'|\boldsymbol{c})$ be the PEP that the adversary codeword $\boldsymbol{c}'$ is selected for the transmitted codeword $\boldsymbol{c}$, the BER union (upper-)bound is given by

$$P_b \quad \leq \quad \frac{1}{(RL - K - 1) 2^{RL-K-1}} \sum_{\boldsymbol{c}, \boldsymbol{c}' \in \mathcal{C}; \boldsymbol{c}' \neq \boldsymbol{c}} A(\boldsymbol{c}, \boldsymbol{c}') P(\boldsymbol{c}'|\boldsymbol{c})$$

where we used the fact that all the codewords are transmitted with equal probabilities.

Since $A(\boldsymbol{c}, \boldsymbol{c}') = A(\boldsymbol{\iota}, \mathbf{0})$ for $\boldsymbol{\iota} = \boldsymbol{c} \oplus \boldsymbol{c}'$, we can simply write it as $A(\boldsymbol{\iota})$ and the union bound in terms of $\boldsymbol{\iota}$ as

$$P_b \leq \frac{1}{(RL-K-1)2^{RL-K-1}} \sum_{\boldsymbol{c} \in \mathcal{C}, \boldsymbol{\iota} \in \mathcal{E}} A(\boldsymbol{\iota}) P(\boldsymbol{c} \oplus \boldsymbol{\iota} | \boldsymbol{c})$$

For ML decision, $P(\boldsymbol{c} \oplus \boldsymbol{\iota} | \boldsymbol{c})$ does not depend on $\boldsymbol{c}$ but only on $\boldsymbol{\iota}$ and can be written as $P(\boldsymbol{\iota})$. Thus, we finally have the following union bound expression in terms of $\boldsymbol{\iota}$ as

$$\begin{aligned} P_b &\leq \frac{1}{RL-K-1} \sum_{\boldsymbol{\iota} \in \mathcal{E}} A(\boldsymbol{\iota}) P(\boldsymbol{\iota}) \\ &= \frac{1}{RL-K-1} \sum_{w=d_f}^{\infty} \sum_{\boldsymbol{\iota} \in \mathcal{E}_w} A(\boldsymbol{\iota}) P(\boldsymbol{\iota}) \end{aligned}$$

where we let $\mathcal{E}_w := \{\boldsymbol{\iota} \in \mathcal{E} | w_H(\boldsymbol{\iota}) = w\}$.

Given an interleaver Ψ, we further introduce a subset of $\mathcal{E}_w$ conditional on the resultant $\mathcal{N}(\boldsymbol{\nu})$, for $\boldsymbol{\nu} = \Psi(\boldsymbol{\iota})$, as

$$\mathcal{E}_w^v := \{\boldsymbol{\iota} \in \mathcal{E}_w | \ |\mathcal{N}(\boldsymbol{\nu})| = v\}$$

which is the set of the weight-w CWEV that give diversity of order of v. Notice $|\mathcal{N}(\boldsymbol{\nu})| \leq w_H(\boldsymbol{\nu}) = w_H(\boldsymbol{\iota})$ and since each subcarrier is maximally capable Q bits, the relationship

$$\left\lceil \frac{w}{Q} \right\rceil \leq v \leq w$$

holds in (7).

The BER union bound (6) is a summation of PEPs, and the inclination of the bound is dominated by the CWEV(s) with the smallest diversity order. Therefore, the *diversity order of the BER bound*, or *diversity order of BER* simply, is given by $\min_{\boldsymbol{\iota} \in \mathcal{E}} |\mathcal{N}(\Psi(\boldsymbol{\iota}))|$ and is upper-bounded by

$$\min |\mathcal{N}(\boldsymbol{\nu})| = \min_{\boldsymbol{\iota} \in \mathcal{E}} |\mathcal{N}(\Psi(\boldsymbol{\iota}))| \leq \min_{\boldsymbol{\iota} \in \mathcal{E}} \{w_H(\boldsymbol{\iota})\} = d_f$$

The union bound is overwhelmed by those terms with the smallest diversity order at sufficiently large SNRs. Thus, if the employed CC is not a pathological one but a standard one as used in the ordinary COFDM, it is reasonable to neglect the contributions of the CWEVs with diversity orders strictly higher than d_f and to approximate the union bound as

$$\begin{aligned} P_b &\leq \frac{1}{RL-K-1} \sum_{w=d_f}^{\infty} \sum_{v=\lceil w/Q \rceil}^{w} \sum_{\boldsymbol{\iota} \in \mathcal{E}_w^v} A(\boldsymbol{\iota}) P(\boldsymbol{\nu}) \\ &\approx \frac{1}{RL-K-1} \sum_{w=d_f}^{Qd_f} \sum_{v=\lceil w/Q \rceil}^{d_f} \sum_{\boldsymbol{\iota} \in \mathcal{E}_w^v} A(\boldsymbol{\iota}) P(\boldsymbol{\nu}) \end{aligned}$$

where $P(\boldsymbol{\nu})$ is upper-bounded by the PEP bound (5) for $\boldsymbol{\nu} = \Psi(\boldsymbol{\iota})$. However, application of (5) needs some preliminary discussions and assumptions.

A. *Approximation for the interleavers with a positive diversity guard*

We introduce the following interleaver class.

Definition 1. For a given interleaver Ψ, we say that a *diversity loss* occurred for a CWEV $\boldsymbol{\iota} \in \mathcal{E}$ if the PEP $P(\boldsymbol{\nu})$, $\boldsymbol{\nu} = \Psi(\boldsymbol{\iota})$, has a diversity order less than d_f, and say that the interleaver has a *diversity guard* (DG) G if it prevent diversity losses for all CWEVs in $\boldsymbol{\iota} \in \cup_{g=0}^{G} \mathcal{E}_{d_f+g}$. We denote the collection of interleavers with DG G as $\boldsymbol{\Psi}_G$.

Conjecture 1. For a certain $G > 0$, the union bound given in (8) can be simplified[4] as

$$P_b \leq \frac{1}{RL-K-1} \sum_{\boldsymbol{\iota} \in \mathcal{E}_{d_f}} A(\boldsymbol{\iota}) P(\boldsymbol{\nu})$$

for each interleaver in $\boldsymbol{\Psi}_G$.

In the followings, we assume the employed interleaver is choosen from $\boldsymbol{\Psi}_G$. Notice that each interleaver in $\boldsymbol{\Psi}_G$, $G \geq 0$, makes $\prod_n w_H(\boldsymbol{\nu}_n) = 1$ for $\boldsymbol{\iota} \in \mathcal{E}_{d_f}$. Thus, by substituting (5) to (9), we have

$$P_b \leq \alpha \sum_{\boldsymbol{\iota} \in \mathcal{E}_{d_f}} \frac{A(\boldsymbol{\iota})}{\det(\boldsymbol{D}(\boldsymbol{\nu}))}$$

[4]The analysis and numerical evidences what provide the conjecture are omitted for limited space.

where the factor α represents all the factors not dependent on $\boldsymbol{\iota}$.

Definition 2. Given a non-reculsive CC with constraint length K, let us call a bit sequence $\boldsymbol{\beta}$ of any length a *base bit sequence* if it begins and ends with 1 and if it does not include $\mathbf{0}_{K-1}$ as a subsequence. A codeword subsequence $\boldsymbol{w}$ of any length is called *base codeword* (BCW) if $(\boldsymbol{w}\ \mathbf{0}_{L-L(\boldsymbol{w})})$ is a codeword for an information vector consisting of a base bit sequence $\boldsymbol{\beta}$ and zero vector as $\left(\boldsymbol{\beta}\ \mathbf{0}_{RL-L(\boldsymbol{\beta})}\right)$, where $L(\boldsymbol{w})$ denotes the length of $\boldsymbol{w}$.

Let $\mathcal{W}$ be the set of all possible BCWs and let $\mathcal{W}_w := \{\boldsymbol{w} \in \mathcal{W}\,|w_H(\boldsymbol{w}) = w\}$. Then, since every elements in $\mathcal{E}_{d_f}$ can be uniquely expressed as

$$\boldsymbol{\iota}_s(\boldsymbol{w}) = (\mathbf{0}_s\ \boldsymbol{w}\ \mathbf{0}_{L-L(\boldsymbol{w})-s}), \quad \boldsymbol{w} \in \mathcal{W}_{d_f},\ 0 \le s \le L - L(\boldsymbol{w})$$

we can rewrite (10) as

$$P_b \le \alpha \sum_{\boldsymbol{w}\in\mathcal{W}_{d_f}} \sum_{s=0}^{L-L(\boldsymbol{w})} \frac{A\left(\boldsymbol{\iota}_s(\boldsymbol{w})\right)}{\det\left(\boldsymbol{D}\left(\Psi(\boldsymbol{\iota}_s(\boldsymbol{w}))\right)\right)}$$

where the weight $A\left(\boldsymbol{\iota}_s(\boldsymbol{w})\right)$ is apparently independent of s and we have writen it simply as $A(\boldsymbol{w})$.

Let $\mathcal{I}(\boldsymbol{w}) := \{i|w_i = 1\}_{i=0}^{L(\boldsymbol{w})-1}$ be the *bit support set* (BSS) of $\boldsymbol{w}$ and assume interleaver Ψ maps the ith bit into the bit position $\psi(i)$. Then, the SSS corresponding to the ICWEV $\boldsymbol{\nu}(s,\boldsymbol{w}) := \Psi(\boldsymbol{\iota}_s(\boldsymbol{w}))$ is given by

$$\mathcal{N}\left(\boldsymbol{\nu}(s,\boldsymbol{w})\right) = \left\{\left\lfloor \frac{\psi(s+i)}{Q} \right\rfloor\right\}_{i\in\mathcal{I}(\boldsymbol{w})}$$

From (4), if we let

$$\boldsymbol{D}_s(\boldsymbol{w}) = \left[\sum_{p=0}^{P-1} W_N^{\left(\left\lfloor \frac{\psi(s+i)}{Q}\right\rfloor - \left\lfloor \frac{\psi(s+i')}{Q}\right\rfloor\right)p} \sigma_p^2\right]_{i\in\mathcal{I}(\boldsymbol{w}),i'\in\mathcal{I}(\boldsymbol{w})}$$

(11) can be rewritten in temrs of BCWs as

$$P_b \le \alpha \sum_{\boldsymbol{w}\in\mathcal{W}_{d_f}} \sum_{s=0}^{L-L(\boldsymbol{w})} \frac{A(\boldsymbol{w})}{\det\left(\boldsymbol{D}_s(\boldsymbol{w})\right)}$$

B. A simplified union bound for almost linear interleavers

For further simplification, we consider (12) under absence of the floor operations. Then, it is trivial that (12) is irrelevant of s if and only if Ψ is LI [15]. For positive integers L and D satisfying $\gcd(L, D) = 1$, an LI Ψ of length L and depth D, denoted by (L, D)-LI, is given by the mapping

$$\psi(i) = [iD]_L$$

and its inverse is specified by $\psi^{-1}(i) = \left[i\bar{D}\right]_L$ for $\bar{D}$ satisfying $[D\bar{D}]_L = 1$, called *complementary number of D over L.*

To consider the influence of the floor operations in the use of LI, we introduce a modulo-Q decomposition of integers as $i = i_1 Q + i_0$, $0 \leq i_0 < Q$. Then, since $\psi(s + i) = [\psi(s) + \psi(i)]_L$, the bits at positions $(s + i)$ and $(s + i')$ are interleaved into the subcarriers with distance

$$\begin{aligned}
& \left\lfloor \frac{\psi(s+i)}{Q} \right\rfloor - \left\lfloor \frac{\psi(s+i')}{Q} \right\rfloor \\
= & \left\lfloor \frac{[\psi(s)+\psi(i)]_L}{Q} \right\rfloor - \left\lfloor \frac{[\psi(s)+\psi(i')]_L}{Q} \right\rfloor \\
= & \left\lfloor \frac{\psi(s)+\psi(i)}{Q} \right\rfloor - \left\lfloor \frac{\psi(s)+\psi(i')}{Q} \right\rfloor \\
= & \left\lfloor \frac{\psi(i)}{Q} \right\rfloor - \left\lfloor \frac{\psi(i')}{Q} \right\rfloor + \left\lfloor \frac{\psi(i)_0+\psi(s)_0}{Q} \right\rfloor - \left\lfloor \frac{\psi(i')_0+\psi(s)_0}{Q} \right\rfloor \\
= & \left\lfloor \frac{\psi(i)}{Q} \right\rfloor - \left\lfloor \frac{\psi(i')}{Q} \right\rfloor + \epsilon(s, i, i')
\end{aligned}$$

where $\epsilon(s, i, i') \in \{0, \pm 1\}$ and the equalities are considered in modulo N.

Let $\boldsymbol{D}(\boldsymbol{w}) = \boldsymbol{D}_0(\boldsymbol{w})$. Then, since

$$\begin{aligned}
\boldsymbol{D}_s(\boldsymbol{w}) &= \left[\sum_{p=0}^{P-1} W_N^{\left(\left\lfloor \frac{\psi(i)}{Q} \right\rfloor - \left\lfloor \frac{\psi(i')}{Q} \right\rfloor + \epsilon(s,i,i') \right) p} \sigma_p^2 \right]_{i \in \mathcal{I}(\boldsymbol{w}), i' \in \mathcal{I}(\boldsymbol{w})} \\
&= \boldsymbol{D}(\boldsymbol{w}) - \left(\sum_{p=0}^{P-1} \sigma_p^2 \right) \boldsymbol{I}_{|\mathcal{I}(\boldsymbol{w})|} + \operatorname{diag} \left(\sum_{p=0}^{P-1} W_N^{\epsilon(s,i,i')p} \sigma_p^2 \right)_{i \in \mathcal{I}(\boldsymbol{w}), i' \in \mathcal{I}(\boldsymbol{w})}
\end{aligned}$$

and

$$\left(\sum_{p=0}^{P-1}\sigma_p^2\right)\boldsymbol{I}_{|\mathcal{I}(\boldsymbol{w})|}-\mathrm{diag}\left(\sum_{p=0}^{P-1}W_N^{\epsilon(s,i,i')p}\sigma_p^2\right)_{i\in\mathcal{I}(\boldsymbol{w}),i'\in\mathcal{I}(\boldsymbol{w})}\approx 0$$

$\det\left(\boldsymbol{D}_s(\boldsymbol{w})\right)\approx\det\left(\boldsymbol{D}(\boldsymbol{w})\right)$ for a sufficiently large N^5. Obviously, the same results holds for the following interleaver class.

Definition 3. If an interleaver Ψ satisfies

$$|[\psi(s+i)]_L-[\psi(s)+\psi(i)]_L|\leq 1,\ \text{if}\ s+i<L$$

it is called *almost linear interleaver* (ALI) and we denote the collection of ALIs as $\boldsymbol{\Psi}_A$.

Finally, for the interleaver class $\boldsymbol{\Psi}_{G,A}:=\boldsymbol{\Psi}_G\cap\boldsymbol{\Psi}_A$, the union bound (13) can be further simplified as

$$P_b\ \leq\ \alpha L\sum_{\boldsymbol{w}\in\mathcal{W}_{d_f}}\frac{A\left(\boldsymbol{w}\right)}{\det\left(\boldsymbol{D}(\boldsymbol{w})\right)}$$

and we can optimize the performance of COFDM by interleavers in the sense to minimize the union bound as

$$\hat{\Psi}=\underset{\Psi\in\boldsymbol{\Psi}_{G,A}}{\arg\min}\,\mathcal{M}\left(\Psi,\mathcal{W}_{d_f}\right)$$

where

$$\mathcal{M}\left(\Psi,\mathcal{W}_{d_f}\right)\ :=\ \sum_{\boldsymbol{w}\in\mathcal{W}_{d_f}}\frac{A\left(\boldsymbol{w}\right)}{\det\left(\boldsymbol{D}(\boldsymbol{w})\right)}$$

It is worth to note that the restriction $s+i<L$ in (14) comes from the fact that, for the zero-padding scheme, there is no CWEV spreads over $(L-1)$th to 0th positions and the (almost) linearity is not required to hold over the positions.

[5]We note that, in the case of LI, $\epsilon(s,i,i')=0$ for BPSK and hence that $\boldsymbol{D}_s(\boldsymbol{w})=\boldsymbol{D}(\boldsymbol{w})$.

V. A Construction of ALI and its Application for COFDM

In this section, we introduce a construction of ALI, proposed in [22], and discuss its parameter selection for COFDM.

A. Construction of ALI

For given integers L and D, $1 \le D < L$, let $C := \gcd(L, D)$, $B := D/C$, $A := L/C$, and $\bar{B}$ be the complimentary number of B over A. We Consider the following mapping and de-mapping rules:

$$\begin{cases} \psi(i) &= [iD + \lfloor i/A \rfloor]_L \\ \psi^{-1}(j) &= [j]_C A + \left[\left\lfloor \dfrac{j}{C} \right\rfloor \bar{B} \right]_A \end{cases}$$

To consider the projection property of (16), we uniquely represent each integer $0 \le i < L$ using the modulo-A decomposition as $i = i_1 A + i_0$, for $0 \le i_0 < A$ and $0 \le i_1 < C$. Then, the mapping rule can be shown as

$$\psi(i) = [(i_1 A + i_0)D + i_1]_L = [i_0 D + i_1]_L = [i_0 B]_A C + i_1$$

and, since A and B are relative prime, the last expression is the modulo-C decomposition which is also unique for each integer in $1 \le j < L$. Thus, the mapping is a bijection and, since $\psi^{-1}(\psi(i)) = i_1 A + \left[i_0 B \bar{B}\right]_A = i$, it can be reversed by the demapping rule. Moreover, by substituting the mapping rule, the left-hand side of (14) can be shown as

$$\begin{aligned} & [\psi(s+i)]_L - [\psi(s) + \psi(i)]_L \\ = \; & [(s+i)_0 D + (s+i)_1]_L - [(s_0 + i_0)D + s_1 + i_1]_L \\ = \; & \begin{cases} 0; & \text{if } s_0 + i_0 < A \\ 1; & \text{if } s_0 + i_0 \ge A \text{ and } s + i < L \end{cases} \end{aligned}$$

Therefore, for each $1 \le D < L$, the interleaver specified by (16) is ALI, named the *ALI with depth-D*, and we denote it as (L, D)-ALI.

Notice that the interleaving specified by (16) includes LI [15] and *block interleaver* (BI) [14] as two special cases, that are cases $\gcd(L, D) = 1$ and D, respectively. Moreover, since $\gcd(L, L-D) = \gcd(L, D)$, the $(L, L-D)$-ALI maps the $(L-i)$th bit to the $[-i_0 D - i_1]_L$th position. Thus, we can see from (12) that, for each $\boldsymbol{\iota}$, (L, D)- and $(L, L-D)$-ALIs give the same $\mathcal{N}(\boldsymbol{\nu})$ and $\boldsymbol{D}(\boldsymbol{\nu})$ in (5). Therefore, the BERs of COFDM are symmetric about the depths.

B. Depth Selection of ALI for COFDM

For a given G, let $\mathcal{D}_G$ be the set of depths which allow the corresponding (L, D)-ALIs to have the DG G. Then, our interleaver design is reduced to the depth selection of ALI as

$$\hat{D} = \arg\min_{D \in \mathcal{D}_G} \sum_{\boldsymbol{w} \in \mathcal{W}_{d_f}} \frac{A(\boldsymbol{w})}{\det(\boldsymbol{D}(\boldsymbol{w}))}$$

where we may let $1 < D \leq L/2$ from its symmetry to reduce searching complexity and the condition $D \in \mathcal{D}_G$ can be verified by whether $|\mathcal{N}(\boldsymbol{\nu})| \geq d_f$ for each $\boldsymbol{\iota} \in \cup_{g=0}^{G} \mathcal{E}_{d_f+g}$.

In COFDM, however, the full diversity order may be obtained only at high SNRs if the subcarriers with indexes $n \in \mathcal{N}(\boldsymbol{e})$ are highly correlative. In order to maximize the diversity order in a moderate SNR region, 1's in $\boldsymbol{\iota}$ should be interleaved into the subcarriers which are low correlative each other. For a fixed $\boldsymbol{\nu}$, we have shown in Sec. III that the diversity order of $\boldsymbol{\nu}$ is determined by $|\mathcal{N}(\boldsymbol{\nu})|$ and from the fact that the subcarrier correlations rely on the *subcarrier spacing* (SS) Δn, we define the following depths set.

Definition 4. For every $\boldsymbol{\iota}_0(\boldsymbol{w})$, $\boldsymbol{w} \in \cup_{g=0}^{G} \mathcal{W}_{d_f+g}$, if an (L, D)-ALI guarantees the existence of a subset $\mathcal{N}'(\boldsymbol{\nu}) \subseteq \mathcal{N}(\boldsymbol{\nu})$, $\boldsymbol{\nu} = \psi(\boldsymbol{\iota}_0(\boldsymbol{w}))$, consisting of d_f entries satisfying

$$|n - n'| \geq \Delta n, \quad \forall n, n' \in \mathcal{N}'(\boldsymbol{\nu}),\ n \neq n'$$

then D is called *G-permissible depth with* Δn. Also, the collection of such depths is denoted as $\mathcal{D}_G(\Delta n)$.

With obove definition, the depth selection of (L, D)-ALI can be modified as

$$\hat{D}(\Delta n) = \underset{D \in \mathcal{D}_G(\Delta n)}{\arg\min} \sum_{\boldsymbol{w} \in \mathcal{W}_{d_f}} \frac{A(\boldsymbol{w})}{\det(\boldsymbol{D}(\boldsymbol{w}))}$$

and the selection given in (18) is the special case of $\Delta n = 1$.

C. Influence of SS on the depth selection

To evaluate the influence of SS Δn on the depth selection, assuming QPSK ($M = 2$) modulated COFDM with $N = 64$, we observed the change of DG G with varing Δn for each depth $1 \leq D \leq 64$. We considered the exponentially decaying Rayleigh fading channels with $\sigma_p^2/\sigma_{p-1}^2 = 0.8$, $1 \leq p < 16$ and employed the rate-$1/2$ feedforward CCs adopted in the IEEE 802.11a [20] and IEEE 802.16e [21]. The constraint lengths, free distances, and generator sequences in octal form of the CCs are listed in Table I.

TABLE I

PARAMETERS OF THE CONSIDERING CCS

Code	K	d_f	$\boldsymbol{g}_0$	$\boldsymbol{g}_1$
I	3	5	5	7
II	5	7	23	35
III	7	10	133	171

The results are summarized in Tables II, III, and IV, for codes I, II, and III, respectively, listed in Table I. In these tables, the depths $1 \leq D \leq 64$ are classified according to supporting DG G for varing SS Δn and those with the same change pattern of G are collected in the same row. For example, we can see from the 4th row on Table II that the depths 14 and 57 support DG $G = 2$ if $\Delta n = 1$. It implies that the (L, D)-ALIs with the depths 14 and 57 interleave the 1's in $\boldsymbol{w}$ into at least $d_f = 5$ distinct subcarriers for all $\boldsymbol{w} \in \cup_{g=0}^{2} \mathcal{W}_{d_f+g}$. Consequently, for the

CWEVs of weights up to $d_f + G = 7$, these depths guarantee the diversity of orders not less than $d_f = 5$ at a high SNR region. This row also implies that if we set $\Delta n = 2$ for obtaining the full diversity order at a moderate SNR region, since the supporting DG G is reduced to 1, the depths 14 and 57 may cause a relative high PEP for some $\boldsymbol{w} \in \mathcal{W}_7$. Notice that although the depths in the same row have the same change pattern of G with the incrasement of Δn, since diversity losses may occur for distinct CWEVs, it does not means the depths in the same row yield the same BER of COFDM.

For a fixed G, on the other hand, we can see from this table that the population of the G-permissible depths $|\mathcal{D}_G(\Delta n)|$ decreases with the increasement of Δn. A small Δn allows some depths in $\mathcal{D}_G(\Delta n)$ interleave 1's in a CWEV into some subcarriers which are highly correlated each other. With increasement of Δn, such depths will be discarded from $\mathcal{D}_G(\Delta n)$ and the depth set becomes empty at a large Δn. As the results, with a small Δn, we can choose a depth from many candidates but the selected depth potentially involves performance losses at a moderate SNR while some proper depths will be discarded from the candidates for a large Δn. In order to find the proper value of SS Δn and to make the depth selection applicable to other cases, in the next subsection, we consider its influence in terms of the *subcarrier correlation ratio of coherent bandwidth* (SCR).

D. Depth selection in terms of SCR

For the exponentially decaying PDP, σ_p^2, $0 \le p \le P-1$, the normalized correlation [3, p. 99] between subcarriers with SS Δn is known as

$$(1 + j2\pi\tau_{\mathrm{rms}}\Delta n/N)^{-1}$$

where $\tau_{\mathrm{rms}} := \sqrt{\sum_{p=0}^{P-1}(p-\bar{p})^2\sigma_p^2}$ for $\bar{p} := \sum_{p=0}^{P-1} p\sigma_p^2$. Thus, we define SCR as

$$t \;:=\; \left[1 + (2\pi\tau_{\mathrm{rms}}\Delta n/N)^2\right]^{-\frac{1}{2}}$$

TABLE II

SUPPORTING G FOR CODE I ("-" STANDS FOR A DG $G < 0$)

<table>
<tr><th>Δn</th><th>1</th><th>2</th><th>3</th><th>4</th><th>5</th><th>6</th><th>7</th><th>8</th><th>9</th><th>10</th></tr>
<tr><td>1,32,43,64</td><td colspan="10">-</td></tr>
<tr><td>16,48</td><td colspan="8">0</td><td colspan="2">-</td></tr>
<tr><td>2,3,26,42,51,63</td><td>2</td><td colspan="9">-</td></tr>
<tr><td>14,57</td><td>2</td><td colspan="6">1</td><td colspan="3">-</td></tr>
<tr><td>18,55</td><td>2</td><td colspan="8">0</td><td>-</td></tr>
<tr><td>21</td><td>2</td><td colspan="9">0</td></tr>
<tr><td>4,5,25,31,33,41,44,52,62</td><td colspan="2">2</td><td colspan="8">-</td></tr>
<tr><td>22</td><td colspan="2">2</td><td colspan="7">0</td><td>-</td></tr>
<tr><td>28</td><td colspan="2">2</td><td colspan="4">1</td><td colspan="4">-</td></tr>
<tr><td>36, 37</td><td colspan="2">2</td><td colspan="6">0</td><td colspan="2">-</td></tr>
<tr><td>6,7,27,45,50,61</td><td colspan="3">2</td><td colspan="7">-</td></tr>
<tr><td>19</td><td colspan="3">2</td><td colspan="6">0</td><td>-</td></tr>
<tr><td>29</td><td colspan="3">2</td><td colspan="3">1</td><td colspan="4">-</td></tr>
<tr><td>54</td><td colspan="3">2</td><td colspan="4">0</td><td colspan="3">-</td></tr>
<tr><td>8,9,24,30,34,40,53,60</td><td colspan="4">2</td><td colspan="6">-</td></tr>
<tr><td>12</td><td colspan="4">2</td><td colspan="2">1</td><td colspan="4">-</td></tr>
<tr><td>15</td><td colspan="4">2</td><td colspan="3">0</td><td colspan="3">-</td></tr>
<tr><td>17,56</td><td colspan="4">2</td><td colspan="4">0</td><td colspan="2">-</td></tr>
<tr><td>20</td><td colspan="4">2</td><td colspan="6">0</td></tr>
<tr><td>47,49</td><td colspan="4">2</td><td colspan="2">0</td><td colspan="4">-</td></tr>
<tr><td>10,11,39,46,59</td><td colspan="5">2</td><td colspan="5">-</td></tr>
<tr><td>35, 58</td><td colspan="5">2</td><td>1</td><td colspan="4">-</td></tr>
<tr><td>23</td><td colspan="5">2</td><td colspan="2">0</td><td colspan="3">-</td></tr>
<tr><td>38</td><td colspan="5">2</td><td colspan="2">0</td><td colspan="3">-</td></tr>
<tr><td>13</td><td colspan="6">2</td><td colspan="4">-</td></tr>
</table>

TABLE III

SUPPORTING G FOR CODE II

<table>
<tr><th>Δn</th><th>1</th><th>2</th><th>3</th><th>4</th></tr>
<tr><td>1,16,32,43,48,51,57,59,64</td><td colspan="4">-</td></tr>
<tr><td>55</td><td>0</td><td colspan="3">-</td></tr>
<tr><td>61</td><td colspan="3">0</td><td>-</td></tr>
<tr><td>8,24,40,56</td><td colspan="4">0</td></tr>
<tr><td>2,3,9,10,13,14,17,18,21,23,25,26,34,35,42,49,58,63</td><td>2</td><td colspan="3">-</td></tr>
<tr><td>29,37</td><td>2</td><td>0</td><td colspan="2">-</td></tr>
<tr><td>6</td><td>2</td><td colspan="2">0</td><td>-</td></tr>
<tr><td>39</td><td>2</td><td>1</td><td colspan="2">-</td></tr>
<tr><td>15,30,50</td><td>2</td><td colspan="3">1</td></tr>
<tr><td>4,5,11,12,20,22,28,31,33,36,38,41,44,46,52,53,60,62</td><td colspan="2">2</td><td colspan="2">-</td></tr>
<tr><td>19,45,47</td><td colspan="2">2</td><td>0</td><td>-</td></tr>
<tr><td>7,27,54</td><td colspan="3">2</td><td>-</td></tr>
</table>

TABLE IV

SUPPORTING G FOR CODE III

<table>
<tr><th>SS</th><th>1</th><th>2</th></tr>
<tr><td>1,8,15,16,17,19,24,27,32,35,39,40,41,43,48,51,53,55,56,57,59,61,64</td><td colspan="2">-</td></tr>
<tr><td>2,3,4,5,6,7,9,10,11,12,13,14,18,21,22,23,25,26,28,29,30,31,33,34,37,38,42,44,45,46,47,49,50,54,58,62,63</td><td>2</td><td>-</td></tr>
<tr><td>4,12,20,28,36,44,52,60</td><td colspan="2">2</td></tr>
</table>

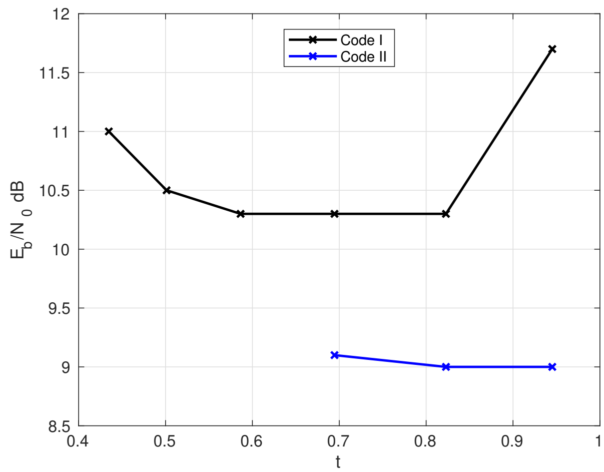

Fig. 2. Required E_b/N_0 for achieving BER 10^{-5}

and, for a given t, corresponding SS can be calculated as

$$\Delta n(t) := \left\lceil \frac{N}{2\pi\tau_{\text{rms}}}\sqrt{\frac{1-t}{t}} \right\rceil$$

To find a proper value of t, in Table V, we let $G = 2$ and listed the depths selected by (19), and for these depths, we compared the required E_b/N_0s to achieve BER 10^{-5} in Fig. 2. Although we could not identify the optimal t from this figure, the optimal t takes value in

TABLE V

THE DEPTHS SELECTED BY (19) WITH $G = 2$

<table>
<tr><td>Δn</td><td>1</td><td>2</td><td>3</td><td>4</td><td>5</td><td>6</td><td>7</td><td>8</td><td>9</td><td>10</td></tr>
<tr><td>$t \times 10$</td><td>9.452</td><td>8.228</td><td>6.945</td><td>5.864</td><td>5.012</td><td>4.347</td><td>3.823</td><td>3.404</td><td>3.063</td><td>2.782</td></tr>
<tr><td>Code I</td><td>21</td><td colspan="3">20</td><td>23</td><td>13</td><td colspan="4">-</td></tr>
<tr><td>Code II</td><td colspan="2">36</td><td>54</td><td colspan="7">-</td></tr>
<tr><td>Code III</td><td colspan="2">28</td><td colspan="8">-</td></tr>
</table>

the rage $0.6 < t_{\text{opt}} < 0.9$. Thus, we let $t = 0.7$ and considered the cases $N = 64$ and 1024

with $P = 16$ and 128, respectively. The selected depths for the exponentially decaying channels $\sigma_p^2/\sigma_{p-1}^2 = 0.8$ and 1, for $1 \leq p < P$ with $\sum_{p=0}^{P-1} \sigma_p^2 = 1$ are listed in Table VI.

TABLE VI

$\hat{D}$ SELECTED BY (19) WITH $G = 2$ AND $t = 0.7$

	Situation 1	Situmation 2	Situation 3	Situation 4
N	64	64	1024	1024
P	16	16	128	128
$\sigma_p^2/\sigma_{p-1}^2$	0.8	1	0.8	1
$\Delta n(0.7)$	2	2	24	3
Code I	20	8	330	16
Code II	36	19	570	16
Code III	28	28	448	16

VI. VALIDITY OF THE CONJECTURE

In the previous section, we have approximated the union bound as

$$\begin{aligned} P_b &\leq \frac{1}{RL-K-1} \sum_{w=d_f}^{Qd_f} \sum_{v=\lceil w/Q \rceil}^{d_f} \sum_{\boldsymbol{\iota} \in \mathcal{E}_w^v} A(\boldsymbol{\iota})\, P(\boldsymbol{\nu}) \\ &= \frac{1}{RL-K-1} \sum_{g=0}^{(Q-1)d_f} \sum_{a=\lceil d_f+g/Q \rceil}^{d_f} \sum_{\boldsymbol{\iota} \in \mathcal{E}_{d_f+g}^a} A(\boldsymbol{\iota})\, P(\boldsymbol{\nu}) \end{aligned}$$

in (8) and simplified the bound as (9) under the conjecture that, for the interleavers with a positive DG G, the contributions of CWEVs $\boldsymbol{\iota} \in \cup_{g=1}^{(Q-1)d_f} \cup_{a=\lceil (d_f+g)/Q \rceil}^{d_f} \mathcal{E}_{d_f+g}^a$ on the bound are negligible.

To consider the validity of the conjecture, we should distinguish the effect of CWEVs $\boldsymbol{\iota} \in \cup_{g=1}^{(Q-1)d_f} \cup_{a=\lceil (d_f+g)/Q \rceil}^{d_f-1} \mathcal{E}_{d_f+g}^a$ and $\boldsymbol{\iota} \in \cup_{g=1}^{(Q-1)d_f} \mathcal{E}_{d_f+g}^{d_f}$. Since the former implies diversity losses on the union BER, the employed interleaver should prevent such events completely. On the other hand, the later affect the accuracy of the simplification, hence (9) keeps its validity if $\left|\bigcup_{g=1}^{(Q-1)d_f} \mathcal{E}_{d_f+g}^{d_f}\right| \ll \left|\mathcal{E}_{d_f}\right|$ holds.

A. The analysis of diversity order

We assume N subcarriers each of which consisting of Q bit positions and, for a weight-w CWEV, consider the occurrence probability of the event $\boldsymbol{\iota} \in \mathcal{E}_w^v$, denoted as $E(w,v)$, under random interleaving argument, that is, given $\boldsymbol{c}$, ψ maps c_0 into a bit position selected with the probability $\frac{1}{QN}$ and maps c_1 into one of the remaining bit positions with probability $\frac{1}{QN-1}$, and so on. Under such random interleaving, every bit, wherever it is, is mapped to each position with the same probability $\frac{1}{QN}$. Then, we can assume $\boldsymbol{\iota} = (\mathbf{1}_w \ \mathbf{0}_{QN-w})$ without loss of generality.

Since $E(w,v)$, $v \leq w$, is the event that the employed interleaver maps $\mathbf{1}_w$ into v subcarriers, it occurs either interleaver maps the last 1 into a subcarrier on which at least one bit has been mapped previously under the event $E(w-1,v)$, or maps it into on an empty subcarrier under event $E(w-1,v-1)$. Thus, we can obtain the following equality

$$\begin{aligned} \Pr\{E(w,v)\} \quad = \quad & \Pr\{E(w,v)|E(w-1,v)\}\Pr\{E(w-1,v)\} \\ & + \Pr\{E(w,v)|E(w-1,v-1)\}\Pr\{E(w-1,v-1)\} \end{aligned}$$

On the other hand, $E(w,v)$ implies that for $QN-w$ empty bit positions, $(N-v)Q$ of them are on the empty subcarriers while remain $vQ-w$ bit positions are on the non-empty subcarriers. Thus, we have the conditional probabilities

$$\begin{cases} \Pr\{E(w+1,v)|E(w,v)\} & = \dfrac{wQ-v}{QN-v} \\ \Pr\{E(w+1,v+1)|E(w,v)\} & = \dfrac{(N-v)Q}{QN-v} \end{cases}$$

By substituting (22) into (21), we derive the following recursive equations as

$$\Pr\{E(w,v)\} \quad = \quad \frac{vQ-w+1}{QN-w+1}\Pr\{E(w-1,v)\} + \frac{(N-v+1)Q}{QN-w+1}\Pr\{E(w-1,v-1)\}$$

and it can be evaluated numerically with the following boundary conditions

$$\begin{cases} \Pr\{E(1,1)\} &= 1 \\ \Pr\{E(w,v)\} &= 0; \quad \text{if } w < v \end{cases}$$

To evaluate the occurrence probability of diversity loss for the CWEVs in $\mathcal{E}_w$, we let $F(w,v)$ be the event that $\mathcal{E}_w^v = \emptyset$ for all CWEVs in $\mathcal{E}_w$, and let $\bar{F}(w,v)$ be the complementary event of $F(w,v)$. Then, since the occurrence probability of $F(w,v)$ is given by

$$\Pr\{F(w,v)\} \;\; = \;\; (1 - \Pr\{E(w,v)\})^{|\mathcal{E}_w|}$$

we have

$$\Pr\{\bar{F}(w,v)\} = 1 - \Pr\{F(w,v)\} \;\; \leq \;\; |\mathcal{E}_w| \Pr\{E(w,v)\} = E\{|\mathcal{E}_w^v|\}$$

where the last inequality can be proved using mathematical induction and is the same with the expection of the population for $\mathcal{E}_w^v$.

B. Numerical results

Assuming QPSK ($Q = 2$) modulated COFDM system with $N = 64$, for the codes in Table I, we listed the populations of BCWs in $\mathcal{W}_{d_f+g}$, $0 \leq g \leq 4$, and the expected number of BCW in $\mathcal{E}_{d_f+g}^{d_f-a}$, $a = 0, 1, 2$, given by (24) in Table VII. We can see from this table that, for each code, the expectation $E\{|\mathcal{E}_{d_f+g}^{d_f-a}|\}$, hence the occurrence probability of the event $\bar{F}(d_f+g, d_f-a)$, is negligibly small as less than 2.0×10^{-4} for $a > 0$ and $g > 2$.

To evaluate the probabilities $\Pr\{\bar{F}(d_f+g, d_f-a)\}$ for large g, for the codes listed in Table I, we shown in Fig. 3 the probabilities $\Pr\{E(d_f+g, d_f-a)\}$ calculated by (23) for $g = 0, 1, 2, 3, 4$.

We can observe from this figure that each curve is concave. This fact implies that, with increasement of g, $\Pr\{E(d_f+g, d_f-a)\}$ tends to 0 faster than exponential order. Thus, if we

TABLE VII

BCWS AND THEIR IMPACT ON $\mathcal{D}_g$

Code	$w_H(\boldsymbol{w})$	$\lvert\mathcal{E}_{d_f+g}\rvert$	$E\left\{\left\lvert\mathcal{E}_{d_f+g}^{d_f}\right\rvert\right\}$	$E\left\{\left\lvert\mathcal{E}_{d_f+g}^{d_f-1}\right\rvert\right\}$	$E\left\{\left\lvert\mathcal{E}_{d_f+g}^{d_f-2}\right\rvert\right\}$	$\lvert\mathcal{D}_g(1)\rvert$
I	5 (g=0)	1	9.2×10^{-1}	7.7×10^{-2}	9.4×10^{-4}	60
	6 (g=1)	2	2.2×10^{-1}	5.6×10^{-3}	1.5×10^{-5}	58
	7 (g=2)	4	2.6×10^{-2}	2.2×10^{-5}	0	58
	8 (g=3)	8	1.7×10^{-3}	3.6×10^{-6}	0	58
	9 (g=4)	16	6.4×10^{-5}	0	0	58
II	7 (g=0)	2	1.7	3.0×10^{-1}	1.3×10^{-2}	55
	8 (g=1)	3	5.8×10^{-1}	3.8×10^{-2}	6.4×10^{-4}	49
	9 (g=2)	4	8.8×10^{-2}	2.5×10^{-3}	1.6×10^{-5}	49
	10 (g=3)	10	1.5×10^{-2}	2.0×10^{-4}	3.4×10^{-7}	49
	11 (g=4)	37	2.6×10^{-3}	1.4×10^{-5}	0	49
III	10 (g=0)	11	7.5	3.1	3.8×10^{-1}	41
	11 (g=1)	0	0	0	0	41
	12 (g=2)	37	2.7	2.3×10^{-1}	7.7×10^{-3}	41
	13 (g=3)	0	0	0	0	41
	14 (g=4)	170	5.4×10^{-3}	4.8×10^{-5}	2.0×10^{-1}	41

over-bound the population of each code as $|\mathcal{E}_{d_f+g}| \leq 2^g |\mathcal{E}_{d_f}|$, we have from (24) the following inequility

$$\Pr\{\bar{F}(d_f+g, d_f-a)\} \leq 2^g |\mathcal{W}_{d_f}| \Pr\{E(d_f+g, d_f-a)\}$$

and since the right-hand side is a decreasing function of g, $\Pr\{\bar{F}(d_f+g, d_f-a)\}$ tends to 0. Therefore, if we employ an interleaver with DG G to prevent the occurrence of diversity losses for CWEVs $\boldsymbol{\iota} \in \mathcal{E}_{d_f+g}$, $g \leq G$, the occrrence probability of diversity losses for CWEVs $\boldsymbol{\iota} \in \mathcal{E}_{d_f+g}$, $g > G$, is vanishingly small and we can suppress the diversity losses on union BER

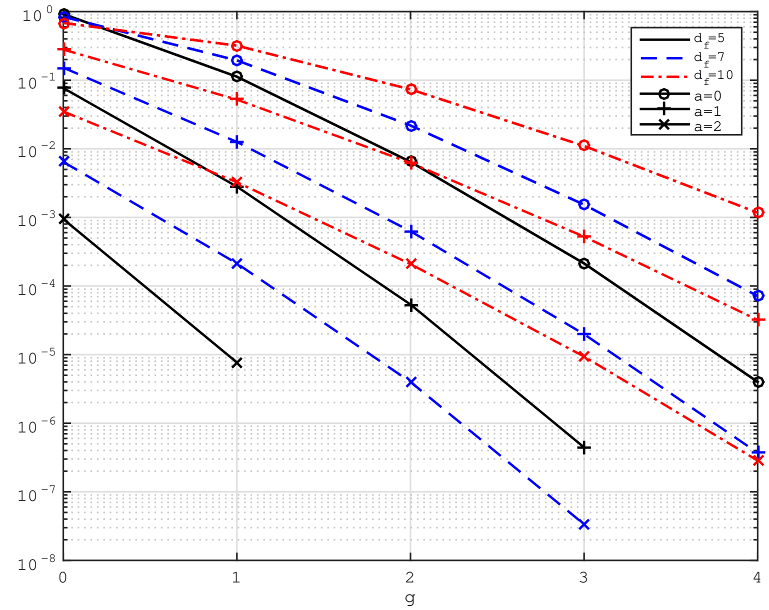

Fig. 3. Occurrence Probabilities of $E(d_f + g, d_f - a)$ for $g = 0, 1, 2, 3, 4$ and $a = 0, 1, 2$

efficiently.

The confirmation is also carried out by observing $|\mathcal{D}_g(1)|$ with varying $0 \leq g \leq (Q-1)(d_f-1)$ for ALI. Table VII lists $|\mathcal{D}_g(1)|$ found in the following manner. We let $\mathcal{D} = \{D\}_{D=1}^{L/2}$ be the initial depth set and, starting from the first BCW in each $\mathcal{W}_{d_f+g}$ for $g = 0$, the depths that yield diversity loss are removed from the set. The process is repeated over the remaining BCWs and for $g = 1$ so on. As shown in Table VII, the size of depth sets are $|\mathcal{D}_2(1)| = 58$, 49, and 41 for codes I, II, and III, respectively. Notice $|\mathcal{D}_g(1)|$ converses to a constant value fast as g increment and remains the value for $g > 2$, and the fact $\mathcal{D}_{d_f}(1) = \mathcal{D}_2(1)$ is confirmed for each code. Therefore, the diversity losses are completely suppressed by use of the ALI with DG $G = 2$.

On the other hand, the ratio of the (expected) number of CWEVs is given by

$$\frac{\left|\mathcal{E}_{d_f}\right|}{\sum_{g=1}^{4} E\left\{\left|\mathcal{E}_{d_f+g}^{d_f}\right|\right\}} = \begin{cases} 4.0 & \text{for} \quad \text{Code I} \\ 2.9 & \text{for} \quad \text{Code II} \\ 3.8 & \text{for} \quad \text{Code III} \end{cases}$$

comparing with $\boldsymbol{\iota} \in \mathcal{E}_{d_f+g}$ for $g > 0$, the contributions of $\boldsymbol{\iota} \in \mathcal{E}_{d_f}$ are dominated part and the approximation of (13) seems acceptable for a practical COFDM with a good designed CC.

Apparently, by taking into account the contribution of the BCWs which result $\mathcal{E}_{d_f+b}^{d_f}$ on the union bound, we can select the depth with more accurate manner. However, the selection of the optimal depth is too complicate and the benefits come from metric modification seems limited.

VII. Simulation results

In this section, the effectiveness of our interleaver design is confirmed by comparison of the BER performances with the ALI for different depths and that with RI and the BI adopted by IEEE industry standard. We also show the superiority of our design by comparisons of BER curves.

A. BER comparisions

In order to verify our depth selection, for the situation 1 in Table VI, we compared BERs at $E_b/N_0 = 7$dB for ALIs with different depths in Figure 4. We obtained each BER plot by accumulating more than 200 bit errors and distinguished G permissible depths with $\Delta n = 2$ for $G < 0$, $G = 0$, and $G = 1$.

We can see from Figure 4 that, for Code I, like at the depths with $G < 0$, the BER performances potentially degrade seriously at the depths with $G = 0$ and 1. For the Codes II and III, even a serious impact does not observed for some depths with $G = 0$ and 1, it may be caused

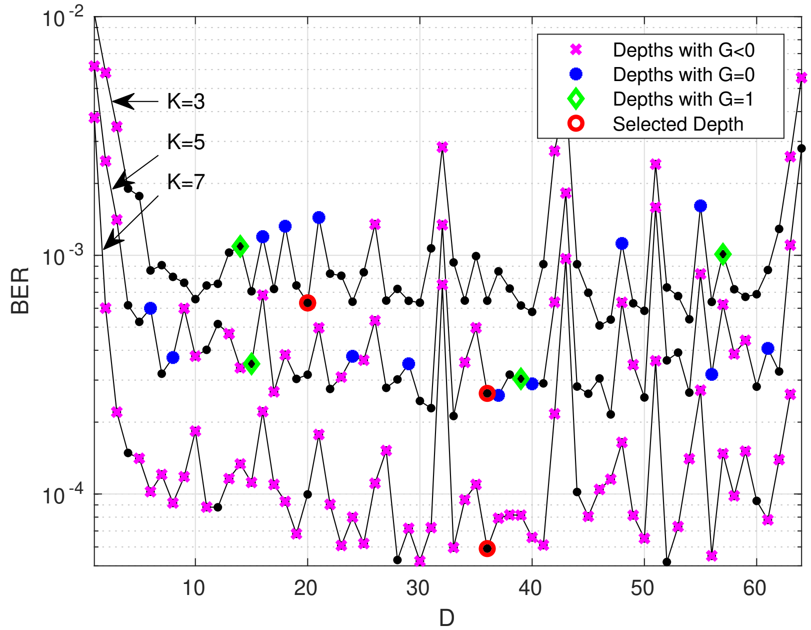

Fig. 4. Metric/BER comparison for Code I

by insufficient SNR, and we suggest discarding these depths from candidates if a low BER is required.

It is worth to note that the optimality of the depth selection is SNR dependent and our design is aimed for the applications working at moderate to high SNR region. Thus, although the ALI with our depth selection does not shown the best BER performance at $E_b/N_0 = 7$dB, it achieves near best performance comparing with other depths.

B. BER comparision

To confirm the effectiveness of our interleaver design, for the situations listed in Table VI, we compared the BER curves of our interleaver design with that of RI[6] and the BIs adopted by

[6]We randomly generated RI but fixed through all simulations.

IEEE industry standards, *i.e.*, $(128, 8)$- and $(2048, 128)$-BIs for $N = 64$ and 1024, respectively, in 5-8. In our simulations, we accumulated more than 2,000 bit errors at each plot.

The superiority of our design to RI and the BI is confirmed for all situations. For these cases, the attainable maximum diversity orders are equal to free distance d_f of the employed CCs, and hence, are 5, 7, and 10, for Code I, II, and III, respectively. For the ALIs with our depth selectin, we can observe the attainability of the maximum diversity orders for Code I and II, while RI and the BI commonly occurs diversity losses. For code III, possibly due to insufficient SNR, we observed a near maximum diversity order 9 in all Figures.

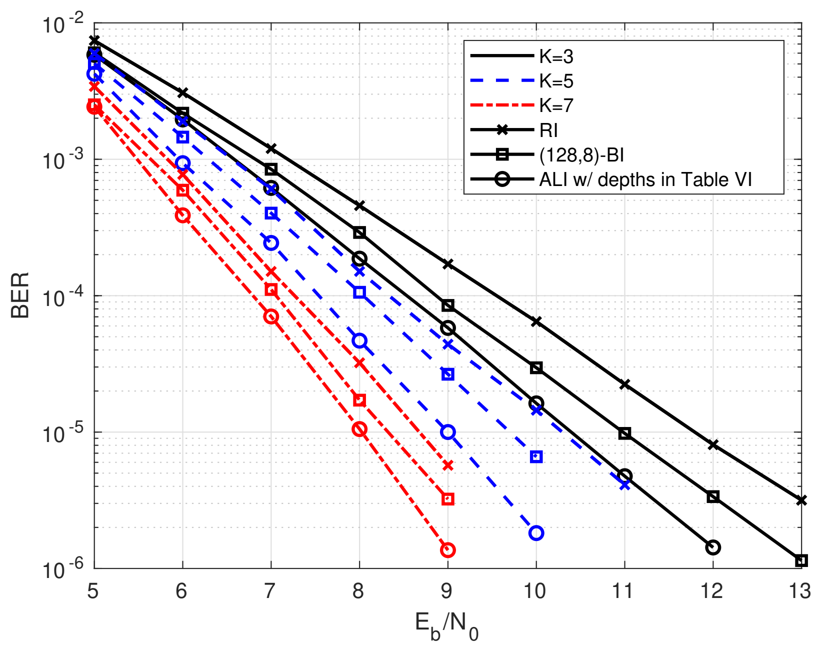

Fig. 5. BER comparison for situation 1

In the case $N = 64$, we can see from Figures 5 and 6 that, to achieve BER 10^{-5}, comparing with the $(128, 8)$-BI, ALI improves E_b/N_0 requirements about 0.6dB, 0.7dB, and 0.3dB observed for situation 1, for codes I, II, and III, respectively, while the requirements are reduced to 0dB, 0.3dB, and 0.2dB for situation 2.

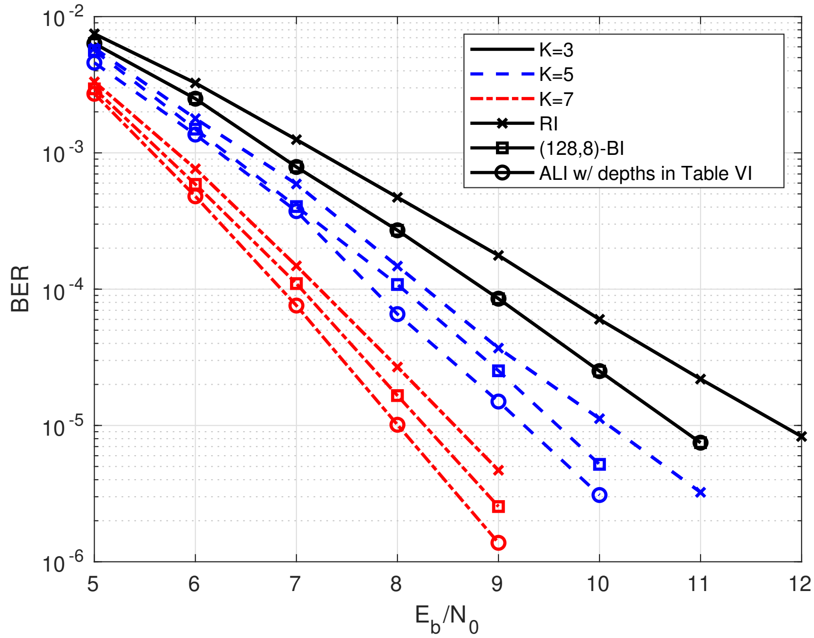

Fig. 6. BER comparison for situation 2

On the other hand, for the case $N = 1024$, although the BI which is widely adopted as industry standards and performs better than RI in situation 3 as shown in Figure 7, we can see from Fig. 8 that the BI performs worse than RI in situation 4 while our design still shows the best performance at a moderate SNR region in both cases.

In situation 3, comparing with the BI, the performance improvement by our designs are about 0.4dB, 0.9dB, and 0.6dB for for codes I, II, and III, respectively, at BER 10^{-5}. In the situation 4, our design improves E_b/N_0 requirements of RI about 0.2dB, 0.1dB, and 0.2dB, for codes I, II, and III, respectively, at BER 10^{-5} and these are increased to about 0.2dB, 0.8dB, and 1.3dB, respectively, for the BI.

Comparing the exponential decaying PDP, the respective interleavers realize a near full diversity on the uniform one and come close to each other in BER curves. We can see from stuation 3 and 4 on Table VI that since the uniform PDP results lower correlation of subchannels than

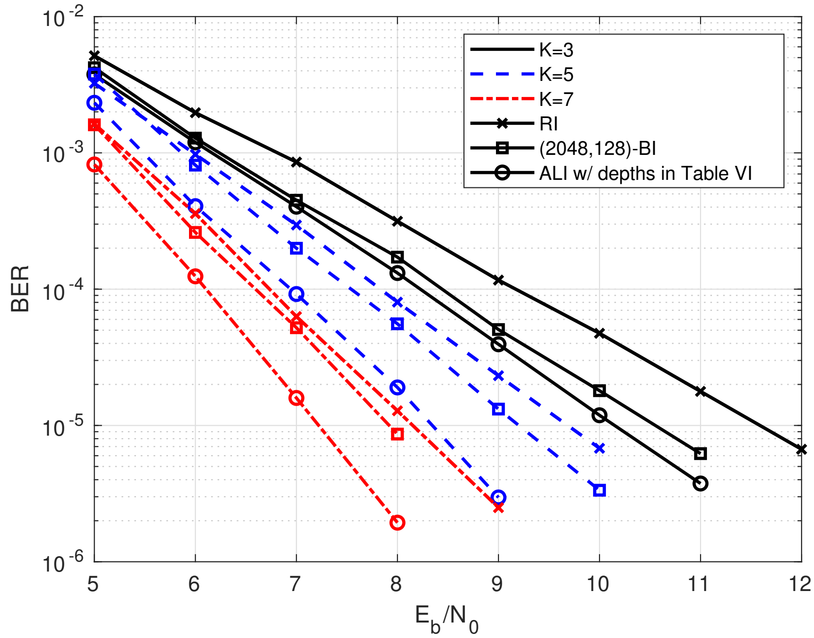

Fig. 7. BER comparison for situation 3

the exponential decaying PDP, it gives more chances to obtain the full diversity order.

VIII. Conclusion

In this paper, we analyzed the BER performance of COFDM and proposed the use of COFDM with ALI. The simulation results shown that our design outperforms the COFDM with RI and the BI adopted by IEEE industry standards.

Appendix

A. Optimality of our decoding rule

Since all-zero initial and final states are assumed, the CC can be regarded as the length-QN block code $\mathcal{C}$. For a given $\boldsymbol{h}$ and $\boldsymbol{r}$, the ML decision $\hat{\boldsymbol{c}}_{\mathrm{ML}}$ and the decision $\hat{\boldsymbol{c}}_{\mathrm{VA}}$ according to our

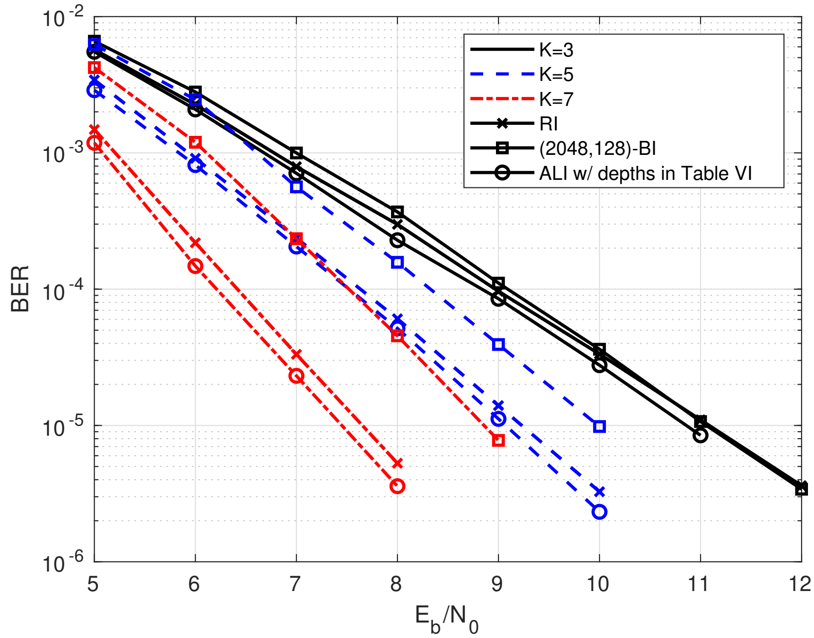

Fig. 8. BER comparison for situation 4

rule with VA can be represented by

$$\begin{cases} \hat{\boldsymbol{c}}_{\mathrm{ML}} & = & \arg\max_{\boldsymbol{c}\in\mathcal{C}} \left\{ \prod_{n=0}^{N-1} P_{\mathrm{ML}}(\boldsymbol{d}_n, \boldsymbol{r}_n) \right\} \\ \hat{\boldsymbol{c}}_{\mathrm{VA}} & = & \arg\max_{\boldsymbol{c}\in\mathcal{C}} \left\{ \prod_{n=0}^{N-1} \prod_{q=0}^{Q-1} P_{\mathrm{VA}}(d_{n,q}, \boldsymbol{r}_n) \right\} \end{cases}$$

where

$$\begin{cases} P_{\mathrm{ML}}(\boldsymbol{d}_n, \boldsymbol{r}_n) & = & C_{\mathrm{ML}}(n) \exp\left(-\frac{|r_n - \mu(\boldsymbol{d}_n)\tilde{h}_n|^2}{N_0} \right) \\ P_{\mathrm{VA}}(d_{q,n}, \boldsymbol{r}_n) & = & \sum_{\boldsymbol{z}\in\{0,1\}^Q | z_q = d_{n,q}} P_{\mathrm{ML}}(\boldsymbol{d}_n, \boldsymbol{r}_n) \end{cases}$$

where $C_{\mathrm{ML}}(n)$ and $C_{\mathrm{VA}}(n)$ are constant values irrelevant to decision.

If all the information bits are mutually independent and equiprobable, we have $\Pr(c_\ell = 0) = \Pr(c_\ell = 1) = 1/2$ for all $0 \leq \ell < QN$, and, for each n, we can write the likelihood function of a length-Q binary vector $\boldsymbol{y}$, for factors $C_{\mathrm{ML}}(n)$ irrelevant to decision, as

$$\begin{aligned}
P_{\mathrm{ML}}(\boldsymbol{y}, r_n) &:= C_{\mathrm{ML}}(n) \exp\left(-\frac{|r_n - \mu(\boldsymbol{y})\tilde{h}_n|^2}{N_0}\right) \\
&= C_{\mathrm{ML}}(n) \exp\left(-\frac{|r_n|^2 + |\mu(\boldsymbol{y})\tilde{h}_n|^2}{N_0}\right) \exp\left(\frac{2\Re\left\{\mu(\boldsymbol{y})\tilde{h}_n r_n^*\right\}}{N_0}\right) \\
&= C'(n) \exp\left(\frac{2\Re\left\{\mu(\boldsymbol{y})\tilde{h}_n r_n^*\right\}}{N_0}\right) \\
&= C'(n) G\left(\mu(\boldsymbol{y}), r_n\right)
\end{aligned}$$

where we let $C'(n) := C_{\mathrm{ML}}(n) \exp\left(-\frac{|r_n|^2 + |\mu(\boldsymbol{y})\tilde{h}_n|^2}{N_0}\right)$ and $G\left(\mu(\boldsymbol{y}), r_n\right) := \exp\left(\frac{2\Re\left\{\mu(\boldsymbol{y})\tilde{h}_n r_n^*\right\}}{N_0}\right)$.

For the QPSK, we have

$$\begin{aligned}
\prod_{q=0}^{1} P_{\mathrm{VA}}(y_q, r_n) &= \prod_{q=0}^{1} \left[\sum_{\boldsymbol{z}\in\{0,1\}^2 | z_q = y_q} P_{\mathrm{ML}}(\boldsymbol{z}, r_n)\right] \\
&= \left[C'(n)\right]^2 \left[G\left(\mu(\boldsymbol{y}), r_n\right) + G\left(j\mu(\boldsymbol{y}), r_n\right)\right] \left[G\left(\mu(\boldsymbol{y}), r_n\right) + G\left(-j\mu(\boldsymbol{y}), r_n\right)\right] \\
&= \left[C'(n)\right]^2 \left\{G\left(\mu(\boldsymbol{y}), r_n\right) \left[G\left(\mu(\boldsymbol{y}), r_n\right) + G\left(j\mu(\boldsymbol{y}), r_n\right) + G\left(-j\mu(\boldsymbol{y}), r_n\right)\right] + 1\right\} \\
&= \left[C'(n)\right]^2 \left\{G\left(\mu(\boldsymbol{y}), r_n\right) \left[\alpha - G\left(-\mu(\boldsymbol{y}), r_n\right)\right] + 1\right\} \\
&= \alpha \left[C'(n)\right]^2 G\left(\mu(\boldsymbol{y}), r_n\right)
\end{aligned}$$

where we let $\alpha := G\left(\mu(\boldsymbol{y}), r_n\right) + G\left(j\mu(\boldsymbol{y}), r_n\right) + G\left(-j\mu(\boldsymbol{y}), r_n\right) + G\left(-\mu(\boldsymbol{y}), r_n\right)$ and used the fact $G\left(\mu(\boldsymbol{y}), r_n\right) G\left(-\mu(\boldsymbol{y}), r_n\right) = 1$ for the last derivation. Comparing (27) and (28), we can conclude that VA coincides ML decision.

REFERENCES

[1] J. A. C. Bingham, "Multicarrier modulation for data transmission: An idea whose time has come," *IEEE Commun. Mag.*, vol. 28, pp. 5–14, May 1990.

[2] A. N. Akansu, O. Duhamel, X. Liu, and M. de Courville, "Orthogonal transmultiplexers in communications: A review," *IEEE Trans. Signal Process.*, vol. 46, no. 4, pp. 979–995, Apr. 1998.

[3] R. V. Nee and R. Prasad, *OFDM for Wireless Multimedia Communications*. Artech House, 2000.

[4] L. Hanzo, M. Munster, B.-J. Choi, and T. Keller, *OFDM and MC-CDMA for Broadband Multi-User Communications*. West Sussex: Wiley, 2003.

[5] B. L. Floch, R. Halbert-Lasalle, and D. Castelain, "Digital sound broadcasting to mobile receivers," *IEEE Trans. Consum. Electron.*, vol. 35, pp. 493–503, Aug. 1989.

[6] P. Höeher, "TCM on frequency selective land mobile fading channels," in *Coded modulation and bandwidth efficient transmission*, E. Biglieri and M. Luise, Eds. Elsevier Science Publisher, 1992.

[7] B. L. Floch, M. Alard, and C. Berrou, "Coded orthogonal frequency division multiplex," *Proc. IEEE*, vol. 83, pp. 982–996, Jun. 1995.

[8] C. Snow, L. Lampe, and R. Schober, "Error rate analysis of coded multicarrier systems over quasi-static fading channels," *IEEE Trans. Commun.*, vol. 55, no. 9, p. 1736–1746, Sep. 2007.

[9] J. Choi, "On the error rate analysis of coded OFDM over multipath fading channels," *IEEE Trans. Wireless Commun. Lett.*, vol. 8, no. 2, pp. 536–539, Apr. 2019.

[10] D. Divsalar and F. Pollara, "Turbo codes for PCS applications," in *Proc. IEEE Int. Conf. Commun. (ICC'95)*, Seattle, WA, Jun. 1995, pp. 54–59.

[11] H. R. Sadjadpour, N. J. A. Sloane, M. Salehi, and G. Nebe, "Interleaver design for turbo codes," *IEEE J. Sel. Areas Commun.*, vol. 19, no. 4, pp. 831–837, May 2001.

[12] C. Fragouli and R. D. Wesel, "Semi-random interleaver design criteria," in *Proc. IEEE Global Telecommun. Conf. (GlobeCom'99)*, Nov. 1999, pp. 2352–2356.

[13] A. Nimbalker, T. E. Fuja, D. J. Costello, T. K. Blankenship, and B. Classon, "Contention-free interleavers," in *Proc. IEEE Int. Symp. Infor. Theory (ISIT2004)*, Chicago, USA, Jun. 2004, p. 52.

[14] L. Perez, J. Seghers, and D. J. C. Jr., "A distance spectrum interpretation of turbo codes," *IEEE Trans. Inf. Theory*, vol. 42, no. 6, pp. 1698–1709, Nov. 1996.

[15] O. Y. Takeshita and D. C. Jr., "New deterministic interleaver designs for turbo codes," *IEEE Trans. Inf. Theory*, vol. 46, no. 2, pp. 1988–2006, Sep. 2000.

[16] C. Berrou, Y. Saouter, C. Douillard, S. Kerouedan, and M. Jezequel, "Designing good permutations for turbo codes: towards a single model," in *Proc. IEEE Int. Conf. Commun. (ICC'04)*, vol. 1, Paris, France, Jun. 2004, pp. 341–345.

[17] J. Sun and O. Y. Takeshita, "Interleavers for turbo codes using permutation polynomials over integer rings," *IEEE Trans. Inf. Theory*, vol. 51, no. 1, pp. 101–119, Jan. 2005.

[18] O. Y. Takeshita, "On maximum contention-free interleavers and permutation polynomials over integer rings," *IEEE Trans. Inf. Theory*, vol. 52, no. 3, pp. 1249–1253, Mar. 2006.

[19] A. Nimbalker, Y. Blankenship, B. Classon, and T. K. Blankenship, "ARP and QPP interleavers for LTE turbo coding," in

Proc. IEEE Wireless Commun. Networking Conf. (WCNC2008), Mar. 2008, pp. 1032–1037.

[20] *Wireless LAN Medium Access Control (MAC) and Physical Layer (PHY) Specifications. High-Speed Physical Layer in the 5 GHz Band*, IEEE 802.11a Std., 1999. [Online]. Available: http://standards.ieee.org/getieee802/802.11.html

[21] *IEEE Standard for Local and Metropolitan Area Networks. Part 16: Air Interface for Fixed Broadband Wireless Access Systems*, IEEE std 802.16-2004 Std., Rev. of IEEE 802.16-2001, Aug. 2004.

[22] C. Han and T. Hashimoto, "Almost linear interleaver and its application in coded OFDM over Rayleigh fading channel," in *Proc. IEEE Int. Symp. Personal, Indoor and Mobile Radio Commun. (PIMRC'13)*, London, U.K., Sep. 2013, pp. 687–692.

[23] J. Proakis, *Digital Communications*, 3rd ed. New York: McGraw-Hill, 1995.

[24] J. W. Craig, "A new, simple and exact result for calculating the probability of error for two-dimensional signal constellations," in *Proc. IEEE Military Commun. Conf. (MILCOM'91)*, vol. 2, McLean, VA, Nov. 1991, pp. 571–575.

[25] M. K. Simon and D. Divsalar, "Some new twists to problems involving the gaussian probability integral," *IEEE Trans. Commun.*, vol. 46, no. 2, pp. 200–210, Feb. 1998.

[26] C. Han, T. Hashimoto, and N. Suehiro, "Constellation-rotated vector OFDM and its performance analysis over Rayleigh fading channels," *IEEE Trans. Commun.*, vol. 58, no. 3, pp. 828–838, Mar. 2010.

[27] S. Galli, "A novel approach to the statistical modeling of wireline channels," *IEEE Trans. Commun.*, vol. 59, no. 5, pp. 1332–1345, May 2011.

[28] L. J. Greenstein, V. E.rceg, Y. S. Yeh, and M. V. Clark, "A new path-gain/delay-spread propagation model for digital cellular channels," *IEEE Trans. Veh. Technol.*, vol. 46, no. 2, pp. 477–485, May 1997.